



# Influence of the non-linearity of fabric tensile behavior for preforming modeling of a woven flax fabric

Christophe Tephany, Damien Soulat, Jean Gillibert, Pierre Ouagne

## ► To cite this version:

Christophe Tephany, Damien Soulat, Jean Gillibert, Pierre Ouagne. Influence of the non-linearity of fabric tensile behavior for preforming modeling of a woven flax fabric. *Textile Research Journal*, 2015, 86 (6), pp.604-617. 10.1177/0040517515595030 . hal-03141826

**HAL Id: hal-03141826**

**<https://hal.science/hal-03141826>**

Submitted on 15 Feb 2021

**HAL** is a multi-disciplinary open access archive for the deposit and dissemination of scientific research documents, whether they are published or not. The documents may come from teaching and research institutions in France or abroad, or from public or private research centers.

L'archive ouverte pluridisciplinaire **HAL**, est destinée au dépôt et à la diffusion de documents scientifiques de niveau recherche, publiés ou non, émanant des établissements d'enseignement et de recherche français ou étrangers, des laboratoires publics ou privés.




## Open Archive Toulouse Archive Ouverte (OATAO)

OATAO is an open access repository that collects the work of Toulouse researchers and makes it freely available over the web where possible

This is an author's version published in: <http://oatao.univ-toulouse.fr/23582>

**Official URL:** <https://doi.org/10.1177/0040517515595030>

### To cite this version:

Tephany, Christophe and Soulat, Damien and Gillibert, Jean and Ouagne, Pierre   
*Influence of the non-linearity of fabric tensile behavior for preforming modeling of a woven flax fabric.* (2015) Textile Research Journal, 86 (6). 604-617. ISSN 0040-5175

Any correspondence concerning this service should be sent  
to the repository administrator: [tech-oatao@listes-diff.inp-toulouse.fr](mailto:tech-oatao@listes-diff.inp-toulouse.fr)

# Influence of the non-linearity of fabric tensile behavior for preforming modeling of a woven flax fabric

© DOI: 10.1177/0040517515595030

Christophe Tephany<sup>1</sup>, Damien Soulat<sup>2</sup>, Jean Gillibert<sup>1</sup> and Pierre Ouagne<sup>1</sup>

## Abstract

The preforming step, which is the first stage of the RESIN Transfer Molding process, has been analyzed by many experimental or numerical approaches in the literature for reinforcements made of synthetic fibers. The complex mechanical behavior of a flax-based plain weave fabric was studied with the view to investigate its formability. Non-linearities in the fabric tensile behavior were observed. A preforming numerical finite element tool was used and validated by performing comparisons between experimental and numerical results. Different tensile behavior models (linear and strongly non-linear) were implemented to investigate their effect on the final shape characteristics. The tool was also used to investigate the effect of the process parameters on the computed preform shape (shear angles and draw-in) for both implemented tensile behaviors. Results show that better correlations take place when using the non-linear tensile behavior. This therefore demonstrates the importance of taking into account non-linearities in the tensile reinforcement behavior while simulating the forming of woven textile reinforcements.

## Keywords

Natural fibers fabrics, preforming, non-linear behavior, process modeling

The mechanical properties of Natural Fiber Composites (NFCs) have been the subject of many review works<sup>1–8</sup> with analyses at different scales. Some authors have focused their works at the scale of individual fibers (microscopic scale), and identified parameters that influence the mechanical behavior in tension.<sup>9–14</sup> In these studies, some of them are focused on non-linear behavior. Placet et al.<sup>11</sup> developed some explanations for hemp fibers, valid at this scale, on the origin of this non-linear tensile behavior. Shah et al.<sup>15</sup> and Baets et al.<sup>16</sup> studied the non-linearity of plant fiber composites. However, if the mechanical behaviors at the scale of the individual fiber and also at the scale of composites are well described, the mechanical behavior of thread, yarns, roving, or dry fabric is less addressed in the literature. Non-linearity in the tensile behavior of quasi-aligned fibers yarns has been underlined in the first part of the load–strain curves.<sup>15</sup> Beyond this, the degree of twisting in yarns<sup>15–18</sup> as well as fiber entanglement in untwisted yarns are the main origins, for low values of load, of the non-linear

zone. At the scale of the fabric, a non-linear zone in the tensile behavior of dry woven fabrics is classically described in the literature, for glass or carbon woven fabrics.<sup>19,20</sup> This phenomenon is due to the woven nature of the preform and especially to the interlacement.<sup>21</sup> Indeed, weaving involves yarn crimp and biaxial behavior.<sup>22</sup> For natural fiber reinforcements loaded in tension, Ouagne et al.<sup>23</sup> showed that the non-linearity zone is consequent.

The subject of this study deals with the importance of taking into account the non-linearity of the fabric tensile behavior for the modeling of the preforming step

---

<sup>1</sup>University of Orleans, France

<sup>2</sup>ENSAIT, France

## Corresponding author:

Pierre Ouagne, University of Orleans, Laboratoire PRISME, 8 Rue Leonard de Vinci, Orléans, 45072 France.  
Email: pierre.ouagne@univ-orleans.fr

of dry or comingled fabrics prior to impregnation by the RTM (RESIN Transfer Molding) or thermo-compression processes. The RTM process consists of injecting a low-viscosity resin in a fibrous reinforcement, initially preformed,<sup>24,25</sup> whereas thermoforming consists of applying simultaneously a temperature and a compaction pressure to the fabric. Previous numerical<sup>26</sup> and experimental<sup>27</sup> studies have shown that forming defects<sup>28–32</sup> may appear and have a strong influence on the resin flow impregnation within the fabric.<sup>33–37</sup> Consequently, performances of the composite part may be seriously impacted.<sup>38,39</sup> To simulate the appearance of these defects during the forming process, the development of appropriate constitutive models that can accurately represent the behavior of textile fabrics resulting from complex reorientation and redistribution of yarn fibers<sup>40</sup> is a main challenge. Due to the multi-scale nature of textiles and despite a lot of research in this field,<sup>41</sup> there is no widely accepted model that describes accurately all the main aspects of fabric mechanical behavior. If some constitutive laws, based on hypoelastic or hyperelastic approaches, take into account non-linearity of the behavior,<sup>40,42–45</sup> the influence of the non-linearity part of the fabric tensile behavior has not been analyzed during the simulation of the preforming step to the author's knowledge.

In this study, a description of the used flax woven fabric and the device to identify the mechanical behavior is first carried out. In the second part, a simple constitutive model of behavior developed in Abaqus software to simulate the preforming stage is described. Comparisons between computed and experimental preforming results are performed to validate the numerical approach and the developed numerical tool has then been used to analyze the importance of taking into account the non-linearity in the fabric tensile behavior for the simulation of the preforming of woven textiles.

## Materials and mechanical characterization

The flax fabric used in this study is a plain weave fabric with an areal weight of  $458 \pm 9 \text{ g/m}^2$ , manufactured by Groupe Depestele (France). The fabric is made of rectangular flat untwisted tows (Figure 1). Before the weaving phase, the fibers were extracted from the stem by following traditional scutching and hackling procedures. As a flat tow approach is used by the manufacturer, the fibers are globally aligned (even if some entanglement can be observed) and a natural binder is used to keep the cohesion of the yarn with the view to support the effort they are submitted to during the weaving phase. No space is visible between the weft tows, whereas the space between the warp tows is  $0.43 \pm 0.09 \text{ mm}$ . The widths of the warp and the weft tows are, respectively,  $2.0 \pm 0.2 \text{ mm}$  and  $2.7 \pm 0.3 \text{ mm}$ .

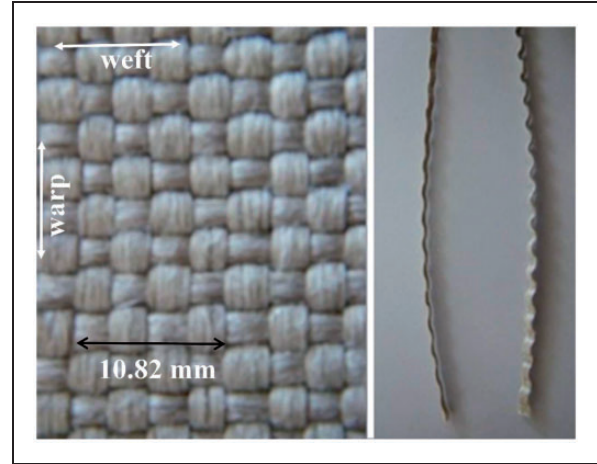
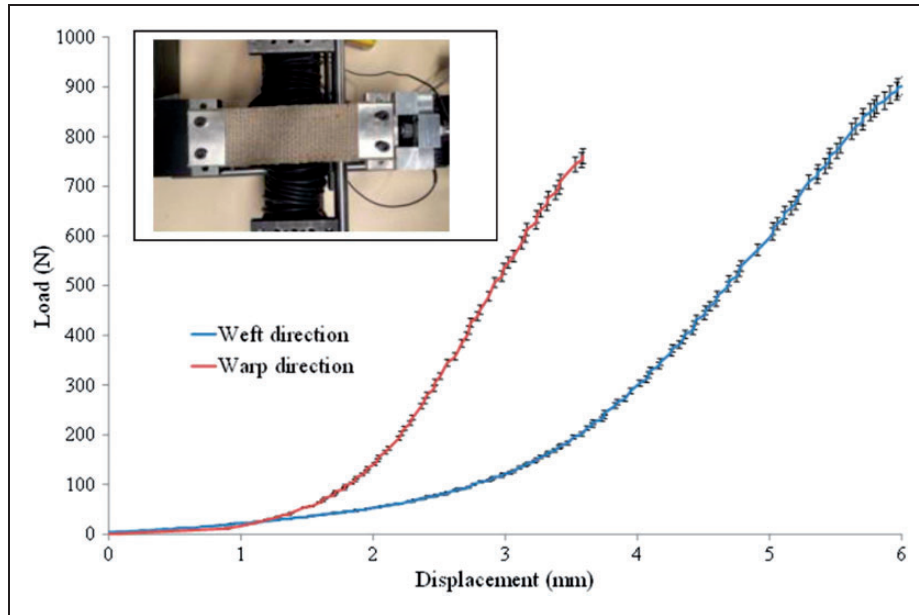


**Figure 1.** The plain weave flax fabric used.

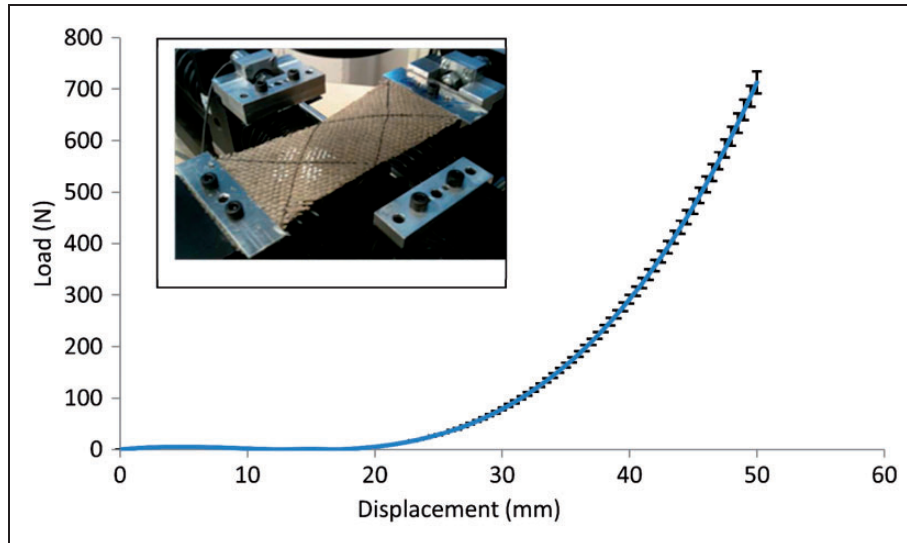
As a consequence, there are 403 warp tows and 370 weft tows per meter of fabric. The linear mass of the warp and the weft tows are, respectively,  $551 \pm 8 \text{ g/km}$  and  $624 \pm 10 \text{ g/km}$ . This fabric has been tested during the preforming step on complex shapes, such as a tetrahedron.<sup>30</sup> In-plane shear is the main deformation mode taking place during draping on a double-curved surface. The in-plane shear mechanical behavior has been intensively studied, mainly using picture frame and bias extension tests.<sup>46,47</sup> To identify the fabric mechanical behavior, uniaxial tensile tests and bias extension tests can be performed. Uniaxial tensile tests are realized at a speed of  $2 \text{ mm/min}$  on samples of  $150 \times 70 \text{ mm}^2$  according to the experimental procedure exposed by Hivet et al.<sup>47</sup> To get rid of slack a pre-tension of  $2 \text{ N}$  is applied to the fabric.

Figure 2 shows the tensile behavior of the fabric in each direction (warp and weft). Each point represented in the curve is the mean values of five tests performed in each direction. The standard deviations are presented in Figure 2. The tensile behaviors of woven fabrics are non-linear mainly because of the woven nature of the fabric that implies crimp. In our case, the non-linear zone is particularly important because a plain weave fabric exhibiting high levels of crimp is used. In the case of this work, the level of crimp is particularly high because almost no space between two adjacent warp or weft yarns is observed.

The constitution and the mechanical behavior of the flax yarns used in this work were studied in detail by Moothoo et al.,<sup>17</sup> who showed that the technical fibers are slightly entangled and therefore not as well aligned as in calibrated synthetic materials. Moreover, the fibers are held together by a natural binder to achieve the cohesion of the flat yarn. As a consequence, the bending stiffness of the flat yarn is higher than that of an equivalent glass or carbon product and this results in



**Figure 2.** Load–displacement curves in warp and weft directions. Picture of the uniaxial tensile test.



**Figure 3.** In-plane shear curve load–displacement with a picture of the bias extension test.

a supplementary increase of the crimp and of the non-linearity levels. The use of natural fiber-based fabric, such as the one presented in this work, therefore implies large crimps that are the main phenomena at the origin of the tensile non-linearity.

Figure 2 also shows the unbalanced behavior of the fabric in both directions. In the weft direction the non-linear behavior is more pronounced than in the warp direction, because these yarns are submitted to more interlacements, which is due to the higher number of warp yarns per unit length. This is the direct consequence of the fact that the warp yarns are of a lower

width than the weft yarns. A higher crimp and therefore a higher non-linearity of the weft yarns tensile behavior take place. Moreover, the slopes of the final linear part of the curves are not identical in each direction.

The in-plane shear behavior was characterized by using the bias extension test on five samples. Figure 3 shows the shear load–displacement curve, with the associated standard deviations. The experimental procedure followed recommendations given in previous studies.<sup>47,48</sup>

In addition to the in-plane characterization phase, sheet forming tests using a hemispherical punch were



performed on a specific device described in Figure 4(a).<sup>49–51</sup> A simple shape was used in this work to validate the numerical model described in the second section of this paper. For the test, a ply of the plain weave flax fabric was placed between the circular blank-holder controlled by four pneumatic jacks that adjust the pressure. In order to monitor the important forming parameters, such as the fabric draw-in, the

in-plane shear, etc., by optical measurements, an “open-die” forming system has been used. Another electric jack imposes the punch displacement. Dimensions of the tools are described in Figure 4(b). For this test, a 0.05 MPa blank-holder pressure was applied (i.e. a load of 625 N) for a displacement of the punch equal to 17.42 mm. Two initial orientations of the fabric denoted by  $0/90^\circ$  and  $\pm 45^\circ$ , specified in Figure 5, have been considered. Material draw-in along the contour and shear angles at selected regions along a path on the deformed fabric have been selected for quantitative comparison between the experimental and the simulated forming tests. A global shape of the preform is presented in Figure 5 with a map of the shear angles measured (with a precision of  $\pm 1^\circ$ ) for each orientation. For the  $0/90^\circ$  orientation (Figure 5(a)), the shear angle zones are numbered and constitute a comparison basis with the simulation results.

### Development of a simulation model taking into account the non-linear behavior

To model fabric draping, different methods based on mapping approaches, such as the kinematical models, were developed. In this model, the yarns are considered inextensible and pin-jointed at crossover points with no relative slippage. The fabric is draped like a “fishnet” on the tool.<sup>52,53</sup> These approaches are fairly efficient, especially in the case of hand-operated draping of classic fabrics or preregs. However, they do not take into account the mechanical behavior of the fabric and the loads on the boundary that can be very important to achieve a correct draping. To analyze the influence of the non-linearity and the unbalanced property of the

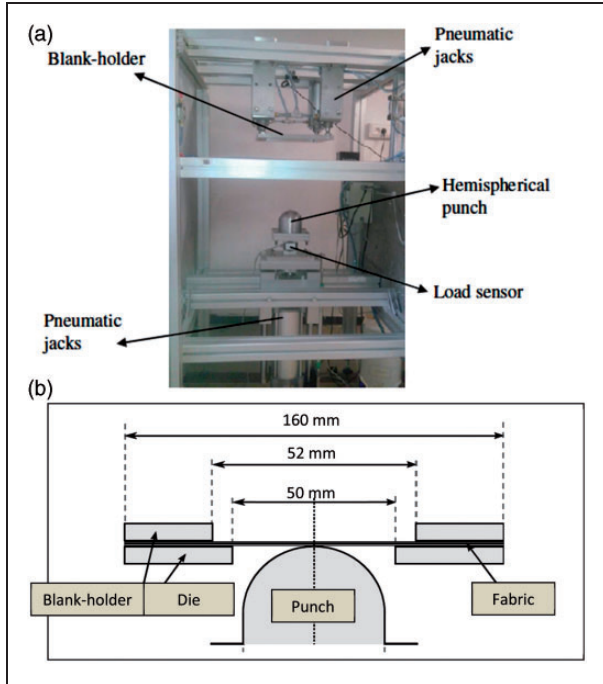


**Figure 4.** Experimental preforming device. (b) Dimensions of the tools.

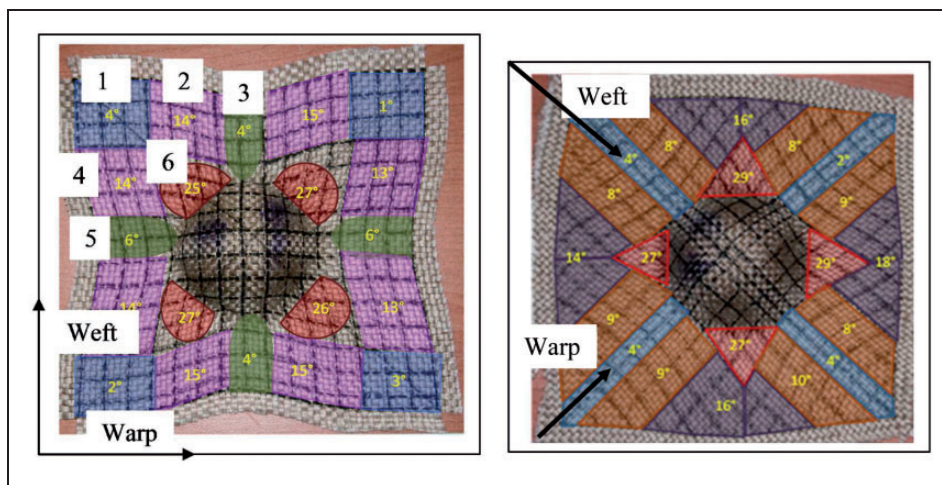


**Figure 5.** Experimental preforming. Global shapes and map of in-plane shear angles measured. (a) Orientation  $0/90^\circ$ . (b) Orientation  $\pm 45^\circ$ .

fabric on the preforming stage, an approach based on the finite element method<sup>26,41</sup> was used.

In the present paper, a simplified method to simulate the preforming process is used with the aims to predict global preform deformation and shear angle distribution with reasonably short calculation times. This method has been developed by Najjar et al.<sup>49,50</sup> It is based on the superposition of a discrete approach to model the tensile behavior and a continuum approach to take into account the in-plane shear behavior and contact with the tools. A “unit cell” (Figure 6) is built using elastic isotropic shell elements and axial connectors between nodes along the edges of the shell element, as opposed to bar and beam elements used by Jauffrés and Sherwood.<sup>54</sup>

In a first approximation, the shell element is considered as isotropic linear elastic and characterized by

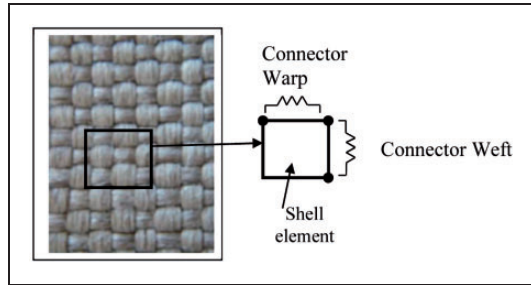


**Figure 6.** Unit cell for the finite element model constituted of a shell element and connectors.

three parameters: shell thickness ( $t$ ), Young’s modulus ( $E$ ), and Poisson’s coefficient ( $\nu$ ). The identification of these parameters for the in-plane shear behavior consists of simulating the bias extension test by the finite element model and determining, by the optimization method, the values that minimize the quadratic error with the experimental curves. Figure 7 shows the result of this procedure in terms of shear simulation load–displacement curves obtained with different values of the Young’s modulus for the shell element. The simulation results are compared to the experimental curves determined from the bias-test. One can demonstrate that the choice of the shell thickness and Poisson coefficient do not have much influence on this in-plane shear behavior.<sup>49,50</sup>

A similar approach was used to identify the rigidity of the connectors associated with the tensile behavior of the fabric. It consists of defining first a model for axial connectors (linking load to displacement). Then simulations of the uniaxial tensile test by the finite element method including these models are carried out before using an optimization procedure to identify the parameters of the model. To study the influence of the non-linearity in the tensile behavior of the fabric, two models are considered.

- A first linear model that associates the connector rigidities to the slopes of linear portions of the experimental load–displacement curves in each direction is defined. This model is thus characterized by two constants denoted by  $K_{warp}$  and  $K_{weft}$ .

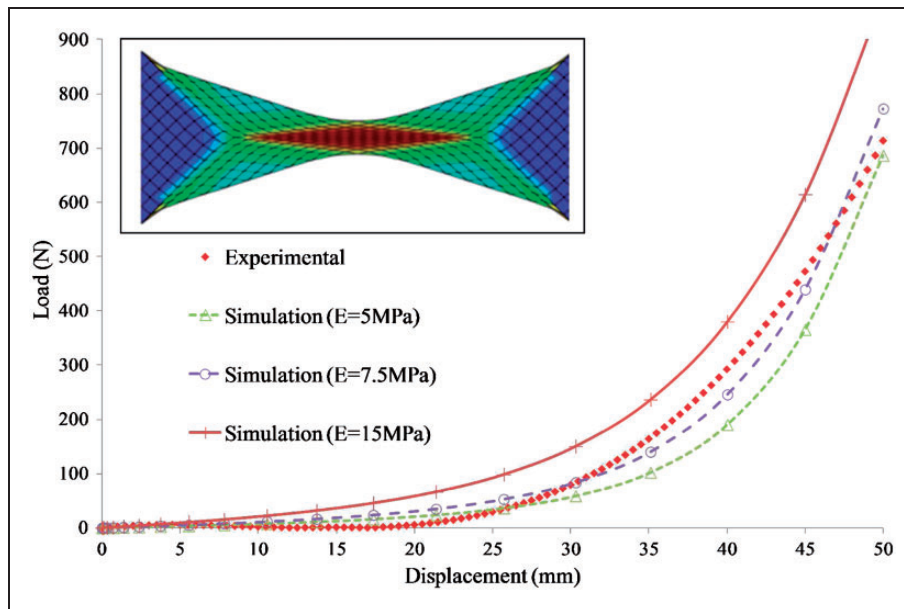


**Figure 7.** Simulation of the bias extension test. Identification of the Young’s modulus for the shell element.

- The second model is non-linear and is divided into two parts, depending on the displacement value; the first polynomial part is a polynomial function of

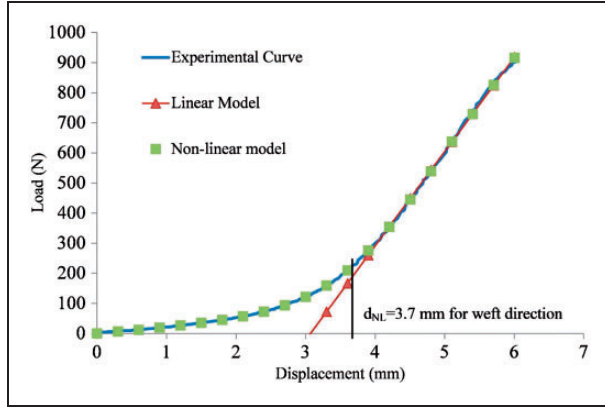


**Figure 8.** Load–displacement curves in the weft direction. Experimental curve and simulation with both models for connectors.

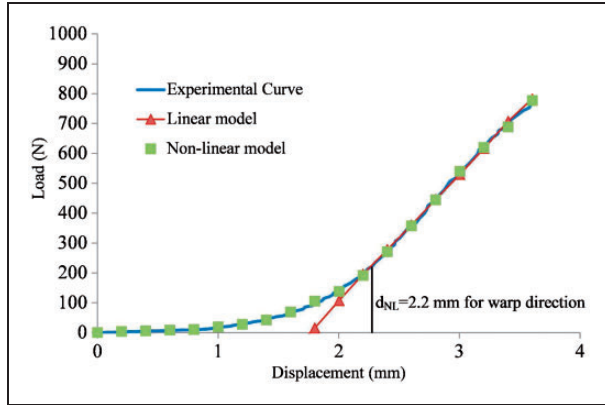


**Figure 9.** Load–displacement curves in the warp direction. Experimental curve and simulation with both models for connectors.

order four, followed by a linear portion (Equation (1)):

$$\begin{aligned} F &= A_1d + A_2d^2 + A_3d^3 + A_4d^4 & \text{for } d \leq d_{NL} \\ F &= A_5d + A_0 & \text{for } d > d_{NL} \end{aligned} \quad (1)$$

where  $F$ ,  $d$ , and  $d_{NL}$  denote respectively the load, the displacement, and the displacement value from which the behavior becomes linear (respectively 3.7 mm for the weft direction, and 2.2 mm for the warp direction, Figure 2).

Figures 8 and 9 show the load–displacement curves obtained by numerical simulation of the uniaxial tensile test, with both models (linear and non-linear), as well as experimental curves, in each direction.

A sensitivity analysis has also been conducted on the influence of the mesh size<sup>55</sup> on the quality of the optimization procedure for the determination of the parameters. For shell elements with four nodes and a size of 1 mm<sup>2</sup>, the optimized values of parameters for the two models are given in Table 1. One can note that the identification procedure has demonstrated that for the warp direction a polynomial of order 3 was obtained ( $A_4 = 0$ ) for the tensile non-linear model.

To check that the tensile behavior is exclusively taken into account by the connectors, elementary tests have been conducted on the simulation of the tensile tests. Figure 10 represents the tensile load–displacement simulation for the weft direction, with the non-linear model associated with the connectors for different values of the Young’s modulus of the shell elements. This test shows that the Young’s modulus, previously determined during the shear parameter identification procedure and chosen for the shell element (7.5 MPa in Figure 7) to model the in-plane shear behavior of the fabric, should be identified carefully. In this case, Figure 10 shows that the simulation data are in good agreement with the experimental values. Choosing other modulus values, such as the high values ones

**Table 1.** Parameters identified for the behavior law in the numerical simulation

Parameters for the in-plane shear behavior (shell element) $E = 7.5 \text{ MPa}$ , $\nu = 0.3$ , $t = 0.1 \text{ mm}$				
Parameters of the connectors	Linear model		Non-linear model	
	Warp (N/mm)	Weft (N/mm)	Warp	Weft
	$K_{warp} = 892$	$K_{weft} = 661$	$A_0 = -10.5 \text{ (N)}$	$A_0 = -13.5 \text{ (N)}$
			$A_1 = 23.E7 \text{ (N/mm)}$	$A_1 = 32.16 \text{ (N/mm)}$
			$A_2 = -21.E5 \text{ (N/mm}^2\text{)}$	$A_2 = 36.46.E2 \text{ (N/mm}^2\text{)}$
			$A_3 = 90.E2 \text{ (N/mm}^3\text{)}$	$A_3 = -32.E4 \text{ (N/mm}^3\text{)}$
			$A_4 = 0. \text{ (N/mm}^4\text{)}$	$A_4 = 13.5E6 \text{ (N/mm}^4\text{)}$
			$A_5 = 892 \text{ (N)}$	$A_5 = 661 \text{ (N)}$



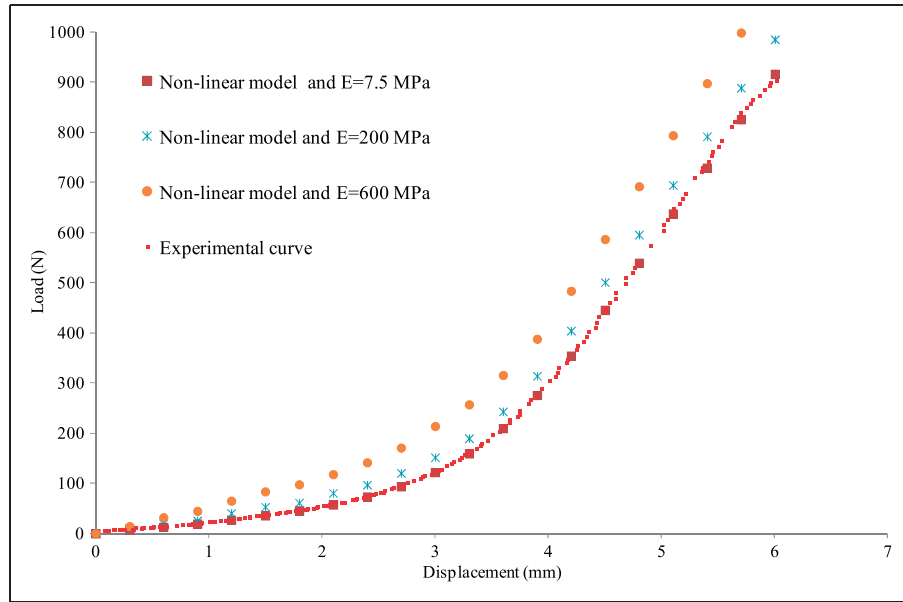


**Figure 10.** Influence of the Young's modulus of the shell element on the tensile response (non-linear model, weft direction).

shown in Figure 10 for the shell elements, may lead to a coupling between the shell and connector elements for the tensile behavior and therefore to inaccurate simulated tensile behaviors, and probably to inaccurate simulations of the forming process.

### Simulation of the forming step

Simulations of the preforming tests have been performed with an explicit solver, in Abaqus software, integrating the behavior laws detailed before for the flax fabric. Tools, whose dimensions are specified in Figure 4(b), are considered to be rigid and the process parameters are the same as the ones used for the experimental tests. Just one layer of the flax fabric is considered. Between the ply and tools, the friction coefficient for the contact is taken to be equal to 0.3, as is commonly used in different preforming studies.<sup>26,29</sup>

#### Tests at constant blank-holder load

For these tests, a constant load equal to 625 N is applied on blank-holders, like in the experimental case. The comparison with experimental tests, described in the first section of this paper, is conducted on the draw-in in each direction (warp and weft) and on the shear angle between yarns. For the 0/90° orientation, Figures 11 and 12 show comparisons between the draw-in computed by both models and experimental measurement points taken respectively in the warp and weft directions. The standard deviation for the experimental measurements of the draw-in is about 0.5 mm.

Figure 11 shows that in the warp direction, the draw-in computed by both models is similar. For the largest draw-in value, the relative difference between the computed and experimental value is about 6%. In the weft direction (Figure 12), the non-linear model is closer to the experimental values. For the largest value of the draw-in, the difference between the experimental one and that computed by the linear model reaches 14%. The maximum draw-in values and the associated relative differences are summarized in Table 2.

The comparison between both models is illustrated in Figures 13 and 14. Figure 13 shows similar results (quasi-superimposed curves) for both directions when the linear models are used. When the non-linear model is used, Figure 14, different results are observed between the warp and the weft directions (~9%). This is in accordance to the unbalanced behavior of the fabric observed experimentally when draw-in is different in the warp and weft directions (~8.5%). This is due to the fact that the waviness of the weft yarns is higher than for the warp ones. As a consequence, the draw-in movement of the weft direction takes place with a delay in comparison to the warp direction and therefore the draw-in, in the weft direction, is lower than in the warp direction. The previous results (Figure 13) confirm that the linear model does not reproduce the unbalanced behavior of the fabric, contrary to the non-linear model, where the draw-in in the warp direction is higher and is well in accordance to the experimental values.

The simulation and experimental shear angles are compared in Table 3 for each area described in Figure 5(a).

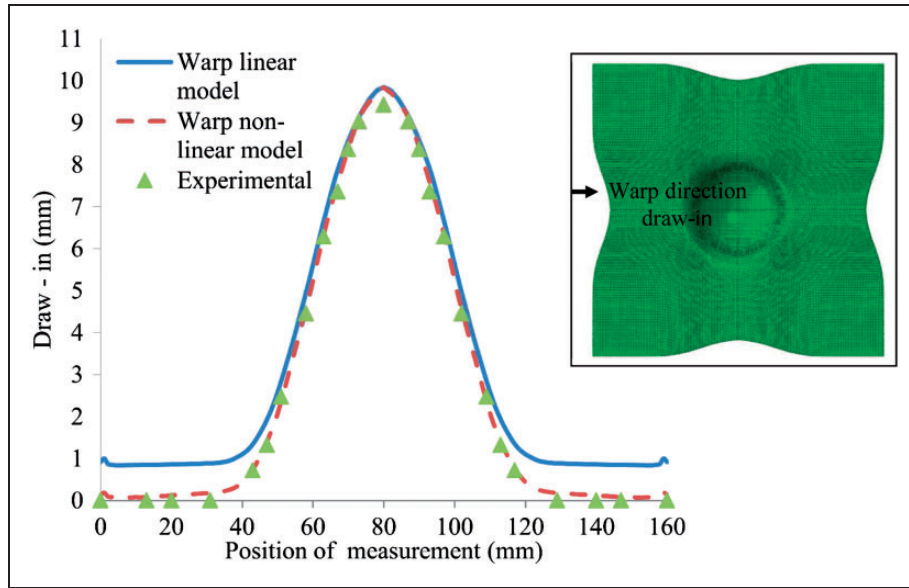


**Figure 11.** Warp direction: comparison between the draw-in computed by both models and the experimental data points.

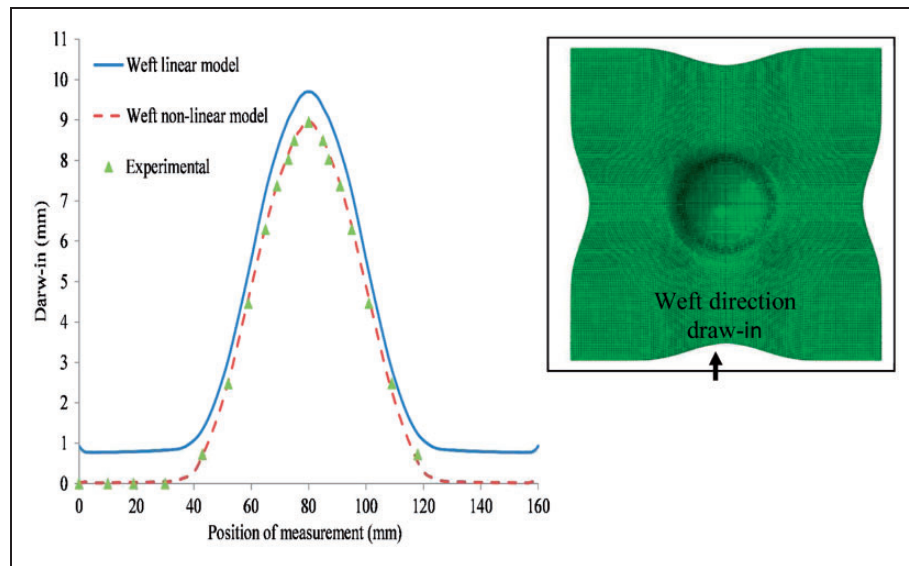


**Figure 12.** Weft direction, comparison between the draw-in computed by both models and the experimental data points.

Table 3 shows that no difference can be observed between the simulation values obtained by the two models. For localized shear angle values one can conclude that both models give almost similar values. They are themselves not significantly different to the experimental values, as they are all situated within the error ranges of experimental and simulation values. All the results, presented in Figures 11–14 and Tables 2 and 3, allow us to validate the non-linear numerical model.

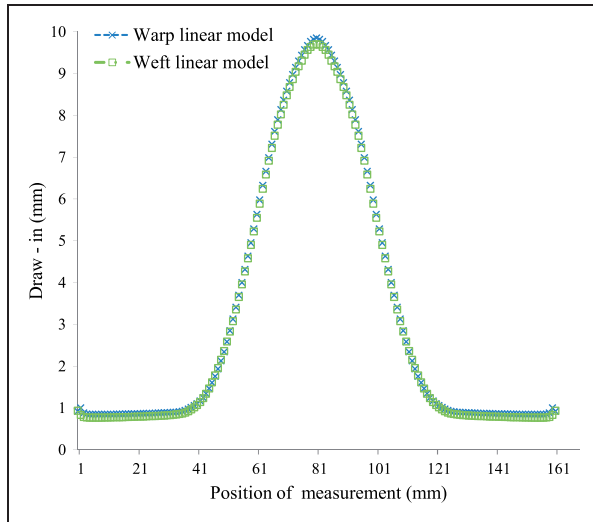
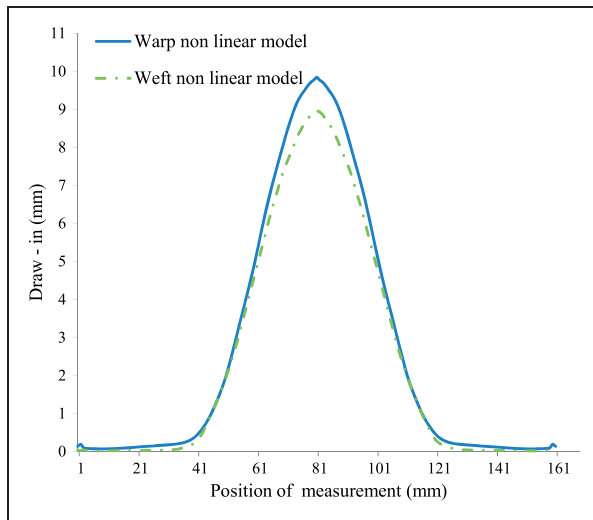
For the  $\pm 45^\circ$  orientation, for the same constant load applied on the blank-holder, Figure 15 compares the

draw-in computed by both models to the experimental values measured on the preform. The outline calculated by the non-linear model best fits the shape of the experimental preform. The difference between both models can reach 9% of the maximum values.

The evolution of the shear angles at  $\pm 45^\circ$  orientation is reported in Figure 16 for both models along a specified edge starting from the top of the hemisphere. Under the punch, the shear angle is null at the top of the hemisphere and reaches maximal values at the location between the die and the blank-holder. Both

**Table 2.** Comparisons of the maximum draw-in for experimental and computed values

	Experimental values $\pm 0.5$ mm	Numerical values (linear model)	Numerical values (non-linear model)	Relative difference expe-model Li Non L	Relative difference between models
Warp direction	9.30 mm	9.85 mm	9.84 mm	-5.9% -5.8%	0.1%
Weft direction	8.50 mm	9.70 mm	8.96 mm	-13.7% -13.6%	7.6%
Relative difference	8.6%	1.5%	8.9%	-	-

**Figure 13.** Draw-in in warp and weft directions computed by the linear model.**Figure 14.** Draw-in in warp and weft directions computed by the non-linear model.**Table 3.** Comparisons of in-plane shear angle between experimental and numerical simulation

Areas	Experimental shear angle values ( $\pm 1^\circ$ )	Numerical shear angle values (linear model) ( $\pm 1^\circ$ )	Numerical shear angle values (non-linear model) ( $\pm 1^\circ$ )
1	4°	2°	2°
2	14°	16°	15°
3	4°	4°	5°
4	14°	16°	16°
5	6°	5°	5°
6	25°	24°	25°

simulation models give, in this zone, relatively similar results. For this test, the difference between the values calculated by the two models is significant at locations between the blank-holder and the die (Figures 16 and 4(b)). At these locations, the load applied by the blank-holder has an influence on the tensile behavior of the fabric, as shown by Capelle et al.<sup>32</sup> and consequently on the level of in-plane shear, especially for this orientation. Values given by the non-linear model are closer to the experimental results given in Figure 5(b).

#### Analysis with variable blank-holder loads

Both numerical models are used to analyze the influence of the load level applied by the blank-holders to the fabric draw-in. For the 0/90 orientation, Figure 17 reports that the maximum value of draw-in decreases as a function of the increasing blank-holder load, for both directions and both models. The linear model, with close values of the draw-in in both directions, does not reproduce the unbalance characteristic of the fabric at any load. On the contrary, the non-linear model reproduces the unbalanced nature of the draw-in. Between both numerical models the difference in draw-in values is higher in the weft direction, where

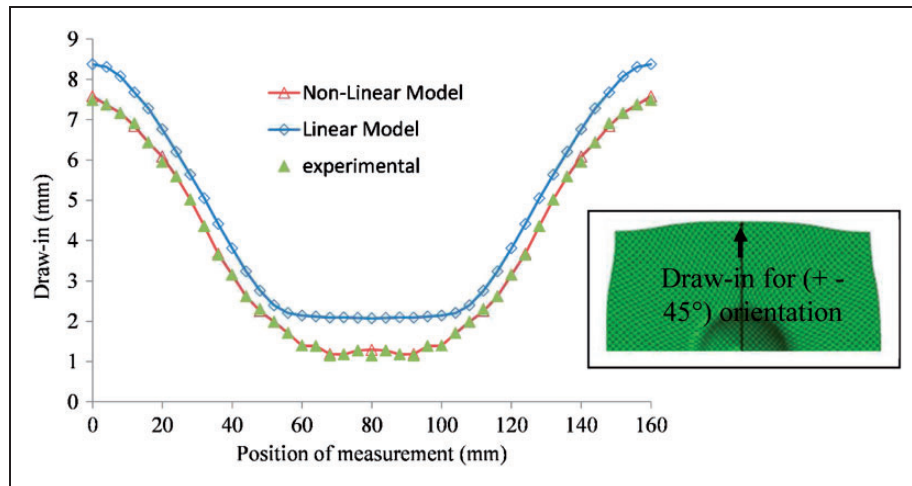


**Figure 15.** Draw-in for  $(\pm 45^\circ)$  orientation: comparison between experimental and computed result by both model values.

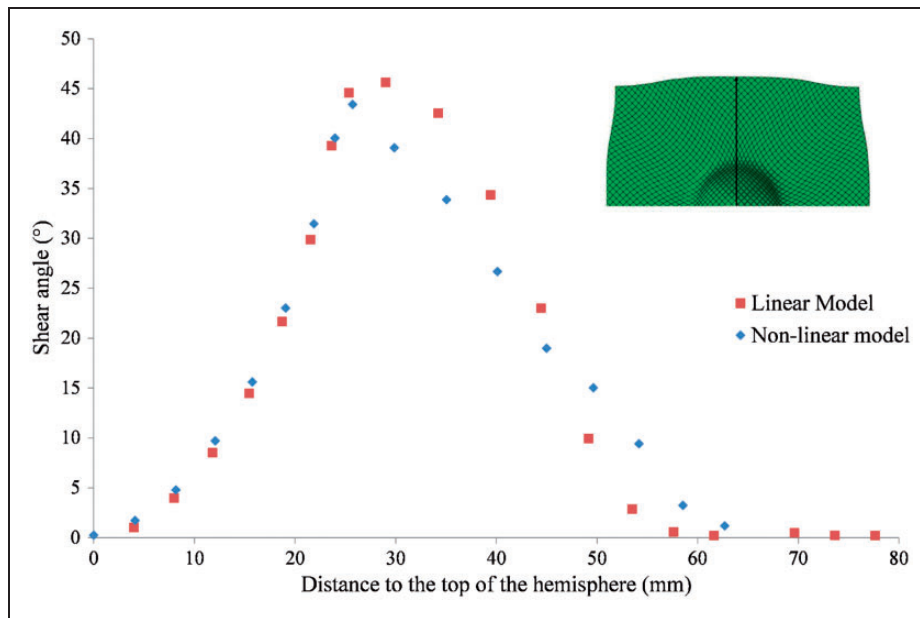


**Figure 16.** Evolution, along the edge, of the shear angle computed with both models.

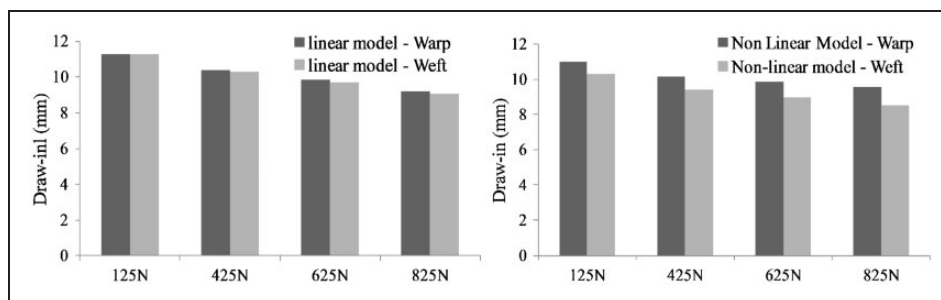


**Figure 17.** Evolution of the simulated maximum values of the draw-in as a function of the load ( $0/90^\circ$ ). Linear and non-linear models.

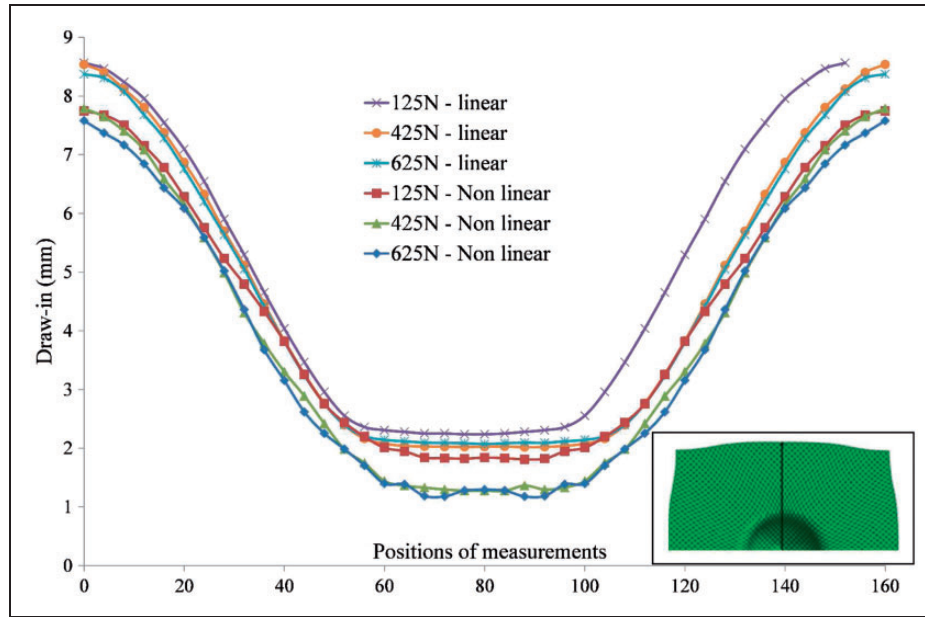


**Figure 18.** Evolution of the draw-in computed with both models for ( $\pm 45^\circ$ ) orientation.

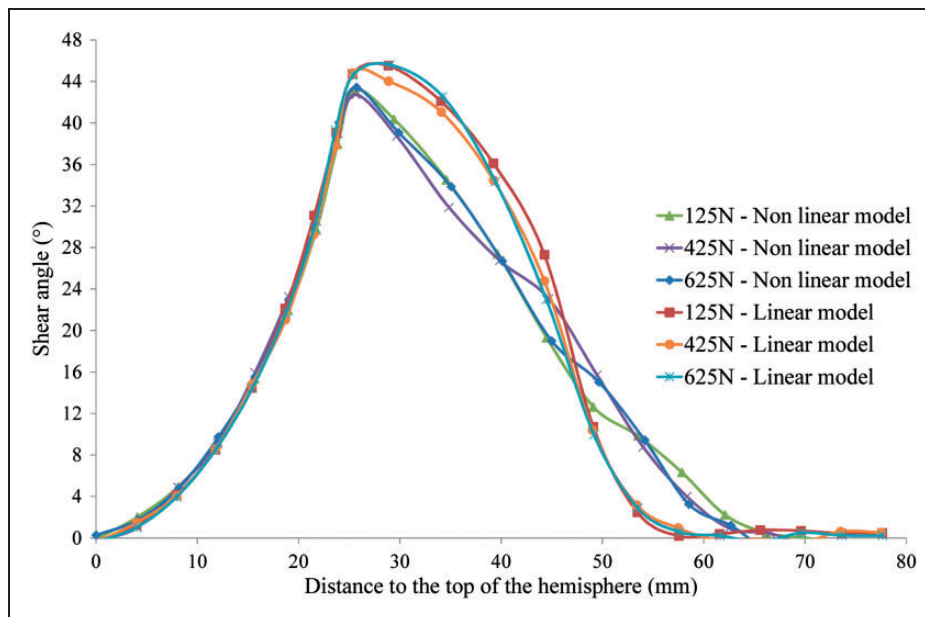


**Figure 19.** Evolution of the shear angle computed with both models in function of the load ( $\pm 45^\circ$ ) orientation.

the non-linearity of the behavior is larger than in the warp direction.

For the  $\pm 45^\circ$  orientation, differences between the draw-in, computed by the linear and the non-linear models, are reported on Figure 18.

For the three values of load considered, the draw-in computed by the linear model is always higher than the one obtained using the non-linear model. This is due to the fact that the rigidity rises previously in the linear

model and, therefore, the draw-in starts earlier than for the non-linear model. This example shows again that it is particularly important to take into account the non-linearity of the tensile behavior of the fabrics.

The influence of the non-linearity in the tensile behavior on the shear angle is described in Figure 19, where the evolution of the shear angle computed by both models along the edge specified in Figure 16 is reported. For the three values of load considered, the



linear model exhibits different values of the shear angles in comparison to the non-linear model, and especially for locations between the die and the blank-holder. As described in the previous section, for the constant load of 625 N, it can be deducted that the tensile behavior has an influence on the magnitude and precision of the shear values. This point has been underlined by Najjar et al.<sup>49,50</sup> for carbon reinforcement. The result presented in Figures 16 and 19 demonstrate that a strong coupling takes place between the in-plane shear and the tensile behavior. Colman et al.<sup>56</sup> and Nosrat-Nezami et al.<sup>57</sup> recently indicated that the coupling between both phenomena should be taken with care in order to obtain accurate preforming simulations. This work therefore shows that the tensile non-linear behavior should be taken into account in order to improve the coupling between the in-plane shear and the tensile behaviors.

## Conclusions

Many papers dealing with natural fibers have dedicated their work to the mechanical behavior at the scale of fibers or yarns. The complexity of the architecture at these scales leads to tensile non-linear behaviors at the scale of the preform. These specific behaviors have an influence during the sheet forming of woven reinforcements. In particular, this work demonstrates that the draw-in and to a lesser extent the shear angle of the reinforcement submitted to hemispherical sheet forming, are particularly sensitive to the tensile behavior non-linearity. For the orientation at  $\pm 45^\circ$ , results shows that the tensile behavior has an influence on the in-plane shear behavior, especially in places close to the load application, while numerical approaches generally dissociate these phenomena. This work therefore demonstrates that the coupling between the in-plane shear and an accurate non-linear tensile behavior should be considered in order to well model the forming of woven preforms showing tensile non-linearity. This phenomenon, in relation to characteristics of reinforcement (fabric architecture, etc.), should be investigated in future works on more complex shapes where stronger tensions are observed.

## Funding

This work was supported by the French environmental agency (ADEME) and the Region Centre.

## References

1. Summerscales J, Dissanayake N, Virk A, et al. A review of bast fibres and their composites. Part 1 – fibres as reinforcements. *Composites Part A* 2010; 41: 1329–1335.
2. Summerscales J, Dissanayake N, Virk A, et al. A review of bast fibres and their composites. Part 2 – composites. *Composites Part A* 2010; 41: 1336–1344.
3. Faruk O, Bledzki AK, Fink HP, et al. Biocomposites reinforced with natural fibers: 2000–2010. *Progr Polym Sci* 2012; 37: 1552–1596.
4. Summerscales J, Virk A and Hall W. A review of bast fibres and their composites: Part 3 – modelling. *Composites Part A* 2013; 44: 132–139.
5. Shah DU. Developing plant fibre composites for structural applications by optimising composite parameters: a critical review. *J Mater Sci* 2013; 48: 6083–6107.
6. Dicker MPM, Duckworth PF, Baker AB, et al. Green composites: a review of material attributes and complementary applications. *Composites Part A* 2014; 56: 280–289.
7. Misnon MI, Islam MdM, Epaarachchi JA, et al. Potentiality of utilising natural textile materials for engineering composites applications. *Mater Des* 2014; 59: 359–368.
8. Dittenber DB and GangaRao HVS. Critical review of recent publications on use of natural composites in infrastructure. *Composites Part A* 2012; 43: 1419–1429.
9. Lefeuvre A, Bourmaud A, Morvan C, et al. Tensile properties of elementary fibres of flax and glass: analysis of reproducibility and scattering. *Mater Lett* 2014; 130: 289–291.
10. Charlet K, Jernot JP, Gomina M, et al. Mechanical properties of flax fibers and of the derived unidirectional composites. *J Compos Mater* 2010; 44: 2887–2896.
11. Placet V, Cissé O and Boubakar ML. Nonlinear tensile behaviour of elementary hemp fibres. Part I: investigation of the possible origins using repeated progressive loading with in situ microscopic observations. *Composites Part A* 2014; 56: 319–327.
12. Trivaudey F, Placet V, Guicheret-Retel V, et al. Nonlinear tensile behaviour of elementary hemp fibres. Part II: modelling using an anisotropic viscoelastic constitutive law in a material rotating frame. *Composites Part A* 2015; 68: 346–355.
13. Kabir MM, Wang H, Lau KT, et al. Tensile properties of chemically treated hemp fibres as reinforcement for composites. *Composites Part B* 2013; 53: 362–368.
14. Thuault A, Bazin J, Eve S, et al. Numerical study of the influence of structural and mechanical parameters on the tensile mechanical behaviour of flax fibres. *J Ind Text* 2014; 44: 22–39.
15. Shah DU, Schubel PJ and Clifford MJ. Modelling the effect of yarn twist on the tensile strength of unidirectional plant fibre yarn composites. *J Compos Mater* 2013; 47: 425–436.
16. Baets J, Plastria D, Ivens J, et al. Determination of the optimal flax fibre preparation for use in unidirectional flax-epoxy composites. *J Reinf Plast Compos* 2014; 33: 493–502.
17. Moothoo J, Allaoui S, Ouagne P, et al. A study of the tensile behaviour of flax tows and their potential for composite processing. *Mater Des* 2014; 55: 764–772.
18. Rask M, Madsen B, Sorensen BF, et al. In situ observations of microscale damage evolution in unidirectional

- natural fibre composites. *Composites Part A* 2012; 43: 1639–1649.
19. Boisse P, Gasser A and Hivet G. Analyses of fabric tensile behaviour: determination of the biaxial tension–strain surfaces and their use in forming simulations. *Composites Part A* 2001; 32: 1395–1414.
  20. Buet-Gautier K and Boisse P. Experimental analysis and modeling of biaxial mechanical behavior of woven composite reinforcements. *Exp Mech* 2001; 41: 260–269.
  21. Mishra S. Influence of distribution of yarn interlacement on uniaxial tensile properties of woven fabrics. *J Text Inst* 2013; 104: 541–549.
  22. Gasser A, Boisse P and Hanklar S. Mechanical behaviour of dry fabric reinforcements. 3D simulations versus biaxial tests. *Comput Mater Sci* 2000; 17: 7–20.
  23. Ouagne P, Soulat D, Tephany C, et al. Mechanical characterisation of flax-based woven fabrics and in situ measurements of tow tensile strain during the shape forming. *J Compos Mater* 2013; 47: 3501–3515.
  24. Advani SG. *Flow and rheology in polymeric composites manufacturing*. Orléans, France, Elsevier, 1994.
  25. Rudd CD and Long AC. *Liquid molding technologies*. Cambridge: Woodhead Publishing Ltd, 1997.
  26. Gereke T, Döbrich O, Hübner M, et al. Experimental and computational composite textile reinforcement forming: a review. *Composites Part A* 2013; 46: 1–10.
  27. Allaoui S, Boisse P, Chatel S, et al. Experimental and numerical analyses of textile reinforcement forming of a tetrahedral shape. *Composites Part A* 2011; 42: 1–10.
  28. Boisse P, Hamila N, Vidal-Sallé E, et al. Simulation of wrinkling during textile composite reinforcement forming Influence of tensile, in-plane shear and bending stiffnesses. *Compos Sci Technol* 2011; 71: 683–692.
  29. Zhu B, Yu TX, Zhang H, et al. Experimental investigation of formability of commingled woven composite preform in stamping operation. *Composites Part B* 2011; 42: 289–295.
  30. Ouagne P, Soulat D, Moothoo J, et al. Complex shape forming of a flax woven fabric; analysis of the tow buckling and misalignment defect. *Composites Part A* 2013; 51: 1–10.
  31. Gatouillat S, Bareggi A, Vidal-Sallé E, et al. Meso modelling for composite preform shaping. Simulation of the loss of cohesion of the woven fibre network. *Composites Part A* 2013; 54: 135–144.
  32. Capelle E, Ouagne P, Soulat D, et al. Complex shape forming of flax woven fabrics: design of specific blank-holder shapes to prevent defects. *Composites Part B* 2014; 62: 29–36.
  33. Walther J, Simacek P and Advani SG. The effect of fabric and fiber tow shear on dual scale flow and fiber bundle saturation during liquid molding of textile composites. *Int J Mater Forming* 2012; 5: 83–97.
  34. Arbter R, Beraud JM, Binetruy C, et al. Experimental determination of the permeability of textiles: a benchmark exercise. *Composites Part A* 2011; 42: 1157–1168.
  35. Hou Y, Comas-Cardona S, Binetruy C, et al. Gas transport in fibrous media: application to in-plane permeability measurement using transient flow. *J Compos Mater* 2013; 47: 2237–2247.
  36. Ouagne P and Bréard J. Continuous transverse permeability of fibrous media. *Composites Part A* 2010; 41: 22–28.
  37. Ouagne P, Ouahbi T, Park CH, et al. Continuous measurement of fiber reinforcement permeability in the thickness direction: experimental technique and validation. *Composites Part B* 2012; 45: 609–618.
  38. Lee SH, Han JH, Kim SY, et al. Compression and relaxation behavior of dry fiber preforms for resin transfer molding. *J Compos Mater* 2010; 44: 1801–1820.
  39. Skordos AA, Aceves CM and Sutcliffe MPF. A simplified rate dependent model of forming and wrinkling of pre-impregnated woven composites. *Composites Part A* 2007; 38: 1318–1330.
  40. Peng X, Guo Z, Diu T, et al. A simple anisotropic hyperelastic constitutive model for textile fabrics with application to forming simulation. *Composites Part B* 2013; 52: 275–281.
  41. Boisse P, Aimène Y, Dogui A, et al. Hypoelastic, hyperelastic, discrete and semi-discrete approaches for textile composite reinforcement forming. *Int J Mater Forming* 2010; 3: 1229–1240.
  42. Khan MA, Mabrouki T, Vidal-Sallé E, et al. Numerical and experimental analyses of woven composite reinforcement forming using a hypoelastic behaviour. Application to the double dome benchmark. *J Mater Proc Technol* 2010; 210: 378–388.
  43. Aimène Y, Vidal-Sallé E, Hagège B, et al. A hyperelastic approach for composite reinforcement large deformation analysis. *J Compos Mater* 2010; 44: 5–26.
  44. Charmetant A, Vidal-Sallé E and Boisse P. Hyperelastic modelling for mesoscopic analyses of composite reinforcements. *Compos Sci Technol* 2011; 71: 1623–1631.
  45. Charmetant A, Orliac JG, Vidal-Sallé E, et al. Hyperelastic model for large deformation analyses of 3D interlock composite preforms. *Compos Sci Technol* 2012; 72: 1352–1360.
  46. Cao J, Akkerman R, Boisse P, et al. Characterization of mechanical behavior of woven fabrics: experimental methods and benchmark results. *Compos Part A* 2008; 39: 1037–1053.
  47. Hivet G, Vidal-Sallé E and Boisse P. Analysis of the stress components in a textile composite reinforcement. *J Compos Mater* 2013; 47: 269–285.
  48. Duquesne S, Samyn F, Ouagne P, et al. Flame retardancy and mechanical properties of flax reinforced woven for composite applications. *J Ind Text* 2015; 44: 665–681.
  49. Najjar W, Legrand X, Pupin C, et al. A simple discrete method for the simulation of the preforming of woven fabric reinforcement. *Key Eng Mater* 2012; 504–506: 213–218.
  50. Najjar W, Legrand X, Dal Santo P, et al. Analysis of the blank holder force effect on the preforming process using a simple discrete approach. *Key Eng Mater* 2013; 554–557: 441–446.
  51. Dufour C, Wang P, Boussu F, et al. Experimental investigation about stamping behaviour of 3D warp interlock composite preforms. *Appl Compos Mater* 2014; 21: 725–738.

52. Van Der Ween F. Algorithms for draping fabrics on doubly curved surfaces. *Int J Numer Method Eng* 1991; 31: 1414–1426.
53. Long AC and Rudd CD. A simulation of reinforcement deformation during the production of preform for liquid moulding processes. *Proc Inst Mech Eng B J Eng Manuf* 1994; 208: 269–278.
54. Jauffrés D and Sherwood JA. Discrete mesoscopic modeling for the simulation of woven-fabric reinforcement forming. *Int J Mater Forming* 2010; 3: 1205–1216.
55. Tephany C, Ouagne P, Soulat D, et al. Simulation of the preforming step for flax dry woven fabrics. In: *16th European conference on composite materials (ECCM16)*, Seville, Spain, 22–26 June 2014.
56. Colman AG, Bridgens BN, Gosling PD, et al. Shear behaviour of architectural fabrics subjected to biaxial tensile loads. *Composites Part A* 2014; 66: 163–174.
57. Nosrat-Nezami F, Gereke T, Eberdt C, et al. Characterisation of the shear–tension coupling of carbon-fibre fabric under controlled membrane tensions for precise simulative predictions of industrial preforming processes. *Composites Part A* 2014; 67: 131–139.